ATLANTIS PRESS

Advances in Engineering Research, volume 150

4th International Conference on Machinery, Materials and Computer (MACMC 2017)

Influences of tooth crack on time-varying mesh stiffness of helical gears

Taoyuan Chen [1], Yanxue Wang [2]

1 School of Mechanical and Electrical Engineering, Guilin University of Electronic Technology, Guilin 541004, PR. China, taoyuan.chen@outlook.com

2 School of Mechanical-Electronic and Vehicle Engineering, Beijing University of Civil Engineering and Architecture, Beijing 100044, PR. China, yan.xue.wang@gmail.com

Keywords: component; helical gear; mesh stiffness; crack model; slicing method

Abstract: The time-varying meshing stiffness (TVMS) provides important information about the health status of the gear system. Tooth faults, like crack, pitting, spalling and breakage will change the TVMS. In order to comprehensively understand the vibration properties of a helical gear set, it is necessary to evaluate the mesh stiffness effectively. In this paper, slicing method, discrete integral method and potential energy method are combined to analytically evaluate the mesh stiffness of a helical gear set. A crack model is developed and the mesh stiffness reduction is quantified when a crack occurs in the pinion or the gear.

1. Introduction

Helical gear mechanism is widely used in the motion and power transmission of various rotating machines due to its advantages of smooth transmission and small impact noise. Time-varying meshing stiffness is one of the main vibration sources of the gear system, especially in the case of gear failure (e.g., spalling, local breakage and root crack). Cracks may occur due to excessive load, improper operation conditions or fatigue of the gear. When a crack occurs, the meshing stiffness of the gear will decrease, and the vibration characteristics of the gear system will change.By reducing the stiffness of different crack levels, the corresponding vibration signals are obtained by dynamic simulation. Vibration signals can be further processed for crack detection and prediction.

A lot of people have developed the time-varying meshing stiffness of spur gears research. Generally speaking, they can be divided into four kinds: finite element method (FEM), analytic method, combination of analytical method and FEM and experimental method. Both the finite element method (FEM) and the analytical method (AM) have been used to evaluate the gear mesh stiffness. But, FEM is complicated and time consuming. While AM can offer a simple and effective way to evaluate the time-varying mesh stiffness. Yang and Lin [1] firstly developed an analytical model to calculate TVMS of a pair of external–external spur gears by considering Hertzian, bending and axial compressive energy. Later, the model was further improved by Tian [2] and Wu [3] by introducing the shearing energy. In the same year,P.Sainsot and P.Velex[4] deduced the influence of wheel body deformation on tooth deformation. And recently Zhou et al. [5] applied this conclusion to the model. The gear was modeled as a cantilever beam from the base circle. Also, Zhou et al. [5], Tian et al. [2], and Pandya and Parey deemed that the gear crack is a linear path starting from the point of intersection of the involute curve and the base circle. Yet in truth the gear tooth starts from the root circle rather than the base circle, which was pointed out by Liang. Chen and Shao [6] proposed an analytical mesh stiffness model based on the crack width along the crack width and the crack depth. Ma and Chen [7] through numerical simulation to establish the dynamic model of gear system's tooth form crack and spalling failure. With the consideration of extended meshing, Ma et al. studied and calculated the root crack or spalling of spur gears with nonlinear contact stiffness of the modified double tooth meshing region and the foundation stiffness. Liang et al. simulated the vibration signal, detected the tooth crack of planetary gear set and calculated tooth pitting gear TVMS. Wan et al. proposed an improved method to calculate TVMS of spur gear with

the potential energy stored in the part between base circle and root circle. Saxena and Parey discovered the influences of spalling and friction on TVMS of spur gears.

For helical gears, a cumulative integral potential energy method was proposed by Wan et al. [8], and the dynamics analysis was carried out. Jiang and Shao studied the effects brought by tooth spalling by assuming a constant per unit of contact length for a single tooth pair. Lin et al.[9] proposed an analytical mesh stiffness model based on tooth spalling and local breakage and studied the influence of spalling shape modification on meshing stiffness.

It is not difficult to see that previous studies focused on spur gears. Compared with the spur gear research, the research of helical gear is far from enough.

The contents of this paper are organized as follows:

Calculation method of time-varying meshing stiffness of helical gears with both healthy tooth and fault defects(crack) is presented in Section 2. Then simulation and discussion are carried out in section 3. Finally draws the conclusion.

2. Mesh stiffness calculation

2.1. TVMS calculation of healthy tooth

In the potential energy method, it is assumed that the total potential energy stored in the meshing gear system consists of four components: Hertzian energy U_h, bending energy U_b , shear energy U_s and axial compressive energy U_a which can be used to calculate Hertzian mesh stiffness k_h, bending mesh stiffness k_b, shear mesh stiffness k_s and axial compressive stiffness k_a, respectively. According to material mechanics and elastic mechanical , U_h, U_b, U_s and U_a can be expressed as follows[8]:

$$U_h = \frac{F^2}{2k_h} \quad (1)$$

$$k_h = \frac{\pi EL}{4(1-\nu^2)} \quad (2)$$

$$U_b = \frac{F^2}{2k_b} = \int_0^d \frac{[F_b(d-x) - F_a h]^2}{2EI_x} dx \quad (3)$$

$$U_s = \frac{F^2}{2k_s} = \int_0^d \frac{1.2F_b^2}{2GA_x} dx \quad (4)$$

$$U_a = \frac{F^2}{2k_a} = \int_0^d \frac{F_a^2}{2EA_x} dx \quad (5)$$

$$I_x = \frac{1}{12}(2h_x)^3 L \quad (6)$$

$$A_x = (2h_x)L \quad (7)$$

where F represents the meshing force between mating gear tooth of pinion and gear in the contact point. Fa , Fb are radial and tangential component forces. G, E, L, v represent shear modulus, Young's modulus, width of tooth and Poisson's ratio, respectively. I_x , A_x represent the area moment of inertia and area of the section where the distance from the dedendum circle is x, the other parameters are shown in Fig. 1(a).

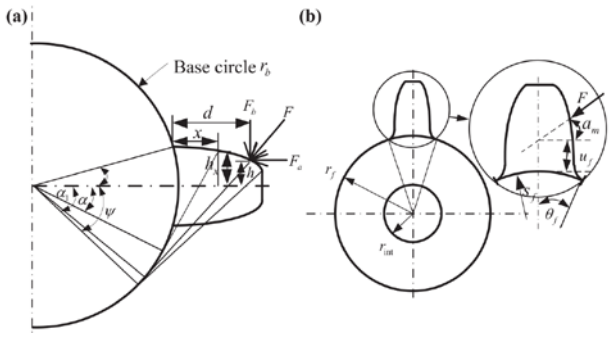

(a) Model of spur gear (b)geometrical parameters

Fig.1.Calculation model of spur gear tooth

When two gears are meshing, the total potential energy stored in a pair of spur gears in mesh can be expressed by:

$$U = \frac{F^2}{2k} = U_h + U_{a1} + U_{b1} + U_{s1} + U_{a2} + U_{b2} + U_{s2} \quad (8)$$
$$= \frac{F^2}{2}\left(\frac{1}{k_h} + \frac{1}{k_{a1}} + \frac{1}{k_{b1}} + \frac{1}{k_{s1}} + \frac{1}{k_{a2}} + \frac{1}{k_{b2}} + \frac{1}{k_{s2}}\right)$$

where k represents the total effective mesh stiffness, subscripts "1" and "2" represent the driving and driven gear, respectively.

Besides the tooth deformation, the fillet-foundation deflection also affects the stiffness of gear tooth. Sainsot, Velex and Duverger [4] proposed an effective method to calculate gear foundation elasticity and the fillet-foundation deflection can be calculated by:

$$\delta_f = \frac{F}{k_f} = \frac{F\cos^2\alpha_m}{Eb}\left\{L*\left(\frac{u_f}{s_f}\right)^2 + M*\left(\frac{u_f}{s_f}\right) + P*\left(1+Q\times\tan^2\alpha_m\right)\right\} \quad (9)$$

The coefficients L, M, P, Q can be approached by polynomial functions

$$X_i(h,\theta_f) = A_i/\theta_f^{\,2} + B_i h^2 + C_i h/\theta_f + D_i h/\theta_f + E_i h + F_i \quad (10)$$

the values of A_i , B_i , C_i , D_i , E_i , F_i are given in reference [8]. L represents the face width. u_f , s_f $h_{fi} = r_f / r_{int}$ and θ_f are defined in Fig. 1(b).In conclusion, for gear teeth in contact, the total effective mesh stiffness can be written as: (11)

$$k = \sum_{i=1}^{n} \frac{1}{\frac{1}{k_{h,i}} + \frac{1}{k_{b1,i}} + \frac{1}{k_{s1,i}} + \frac{1}{k_{f1,i}} + \frac{1}{k_{a1,i}} + \frac{1}{k_{b2,i}} + \frac{1}{k_{s2,i}} + \frac{1}{k_{a2,i}} + \frac{1}{k_{f2,i}}}$$

where subscripts "1" and "2" denote the pinion and gear respectively, and n represents the number of the gear tooth meshing at the same time.

However, unlike the spur gears, the engaging-in and engaging-out of helical gears are a gradual process. The length of the contact line gradually changes from zero to maximum and then from zero to maximum. Accordingly, the TVMS is also gradually changing from zero to maximum and then from zero to maximum. Obviously, due to the existence of spiral angle and axial force, the meshing stiffness of helical gear can not be calculated as the meshing stiffness of spur gear. Wan et al. [8] proposed a method to separate helical gears into a series of independent sheets with thickness of dy. Then the helical gear is considered as a series of crossed gears without elastic coupling, because the narrow tooth gear is usually negligible. Then, the stiffness of the whole tooth is obtained by integrating the width of the tooth surface. Finally, the following formula is obtained.

(12)

$$k_b = \sum_{1}^{N} \frac{1}{\int_{-\alpha_1'}^{\alpha_2} \frac{3\left\{1+\cos\alpha_1'\left[(\alpha_2-\alpha_1')\sin\alpha-\cos\alpha\right]\right\}^2(\alpha_2-a)\cos\alpha}{2E\left[\sin\alpha+(\alpha_2-\alpha)\cos\alpha\right]^3}d\alpha}\Delta y$$

(13)

$$k_s = \sum_{1}^{N} \frac{1}{\int_{-\alpha_1'}^{\alpha_2} \frac{1.2(1+\nu)(\alpha_2-a)\cos\alpha\cos^2\alpha_1}{E\left[\sin\alpha+(\alpha_2-\alpha)\cos\alpha\right]}d\alpha}\Delta y$$

(14)

$$k_a = \sum_{1}^{N} \frac{1}{\int_{-\alpha_1'}^{\alpha_2} \frac{(\alpha_2-a)\cos\alpha\sin^2\alpha_1}{2E\left[\sin\alpha+(\alpha_2-\alpha)\cos\alpha\right]}d\alpha}\Delta y$$

where $\alpha_1' = \alpha_1 + (\varphi - \alpha_1)(i/N)$. N is the number of pieces which the helical gear is divided into. Δy denotes width of each piece. For the detailed derivations of the above expressions, refer to the reference [9] please.

2.2. TVMS calculation of tooth with crack

The tooth crack usually starts at the point where the maximum stress is in the material. Lewicki shows that the crack propagation path is smooth, continuous, and in most cases only slight bending and straight. It is assumed that a cracked tooth is still regarded as a cantilever beam, and the depth of the crack is linearly varied along the width of the surface, as shown in Figure 2. These cracks are then described as functions of crack length and crack depth:

$$q(u) = \begin{cases} q - \frac{q}{L_c}u & L_c < L \\ q - \frac{q-q_0}{L}u & L_c = L \end{cases} \quad (15)$$

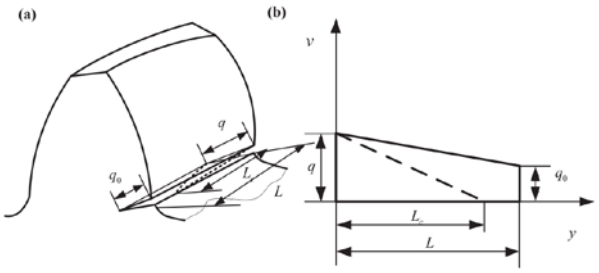

Fig.2.Cracked tooth model of helical gears

As shown in Fig. 3, a cracked gear tooth is divided into many thin sections. One of the explanations is chosen to calculate the meshing stiffness of the spiral line with a crack. Because the profile curve is perfect, the contact stiffness k_h and the axial compressive stiffness k_a will not change. However, the crack will change the bending and shear stiffness[10]. When the crack exists, according to Formula (16) and (17), the distance between the inertia of the x section and the effective area of the area will be calculated from the tooth root distance.

$$dI_x = \begin{cases} \frac{1}{12}(h_c + h_x)^3 dy & x \le g_c \\ \frac{1}{12}(2h_x)^3 dy & x > g_c \end{cases} \quad (16)$$

$$dA_x = \begin{cases} (h_c + h_x)dy & x \le g_c \\ 2h_x dy & x > g_c \end{cases} \quad (17)$$

According to the different conditions, the corresponding formula of bending and shear stiffness under the crack condition can be obtained.

a. When $h_c < h_r$ or when $h_c \ge h_r$ & $\alpha_1 \le \alpha_g$

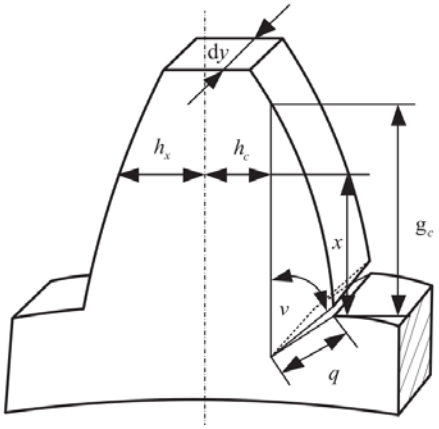

Fig.3. A thin pieces of cracked tooth model

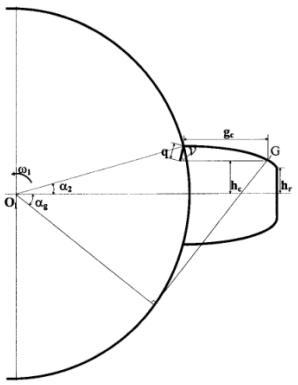

Fig.4. A thin Section of cracked tooth model

As shown in Figure 4, h_r is half of the roof chordal tooth thickness. In this case ,x shown in Figure 3 is always less than or equal to g_c. Thus I_x and A_x should be calculated as follows:

$$dI_x = \frac{1}{12}\{R_{b1}[\sin\alpha_2 + (\alpha+\alpha_2)\cos\alpha - \sin\alpha] - q(y)\sin\nu(y)\}^3 dy \quad (18)$$

$$dA_x = \{R_{b1}[\sin\alpha_2 + (\alpha+\alpha_2)\cos\alpha - \sin\alpha] - q(y)\sin\nu(y)\}dy \quad (19)$$

Substituting Equation. (18) and (19) into Equation.(3) and (4) respectively, then integrating the width along the width, the bending stiffness K is obtained.

(20)

$$k_b^{\,c} = \int_0^L \frac{1}{\int_{-\alpha_1}^{\alpha_2} \frac{12\{1+\cos\alpha_1[(\alpha_2-\alpha)\sin\alpha-\cos\alpha]\}^2(\alpha_2-\alpha)\cos\alpha}{EL\left[\sin\alpha_2-\frac{q(y)}{R_{b1}}\sin\nu(y)+\sin\alpha+(\alpha_2-\alpha)\cos\alpha\right]^3}d\alpha}dy$$

(21)

$$k_s^{\,c} = \int_0^L \frac{1}{\int_{-\alpha_1}^{\alpha_2} \frac{2.4[1+\nu(y)](\alpha_2-\alpha)\cos\alpha\cos^2\alpha_1}{EL\left[\sin\alpha_2-\frac{q(y)}{R_{b1}}\sin\nu(y)+\sin\alpha+(\alpha_2-\alpha)\cos\alpha\right]}d\alpha}dy$$

Applying discrete integral method, the stiffness could be calculated by

(22)

$$k_b^{\,c} = \sum_1^N \frac{1}{\int_{-\alpha_1}^{\alpha_2} \frac{12\{1+\cos\alpha_1[(\alpha_2-\alpha)\sin\alpha-\cos\alpha]\}^2(\alpha_2-\alpha)\cos\alpha}{EL\left[\sin\alpha_2-\frac{q(y)}{R_{b1}}\sin\nu(y)+\sin\alpha+(\alpha_2-\alpha)\cos\alpha\right]^3}d\alpha}\Delta y$$

(23)

$$k_s^{\,c} = \sum_1^N \frac{1}{\int_{-\alpha_1}^{\alpha_2} \frac{2.4[1+\nu(y)](\alpha_2-\alpha)\cos\alpha\cos^2\alpha_1}{EL\left[\sin\alpha_2-\frac{q(y)}{R_{b1}}\sin\nu(y)+\sin\alpha+(\alpha_2-\alpha)\cos\alpha\right]}d\alpha}\Delta y$$

b. When $h_c \geq h_r$ & $\alpha_1 > \alpha_g$

In this case, the contact point of a pair of mating gears on the tooth profile will be located between point G and the tooth roof. The total integrations for calculations of k_b and k_s will consist of two parts respectively. The first part, corresponding to $\alpha \leq \alpha_g$, can be calculated by Equation.(18) and (19) respectively. The second part, corresponding to $\alpha > \alpha_g$, can be calculated by Equations(16) and (17). Therefore, the bending and shear stiffness will be equal to the summation of these two parts as follows.

(24)

$$k_b^{\,c} = \int_0^L \frac{1}{\int_{-\alpha_g}^{\alpha_2} \frac{12\{1+\cos\alpha_1[(\alpha_2-\alpha)\sin\alpha-\cos\alpha]\}^2(\alpha_2-\alpha)\cos\alpha}{EL\left[\sin\alpha_2-\frac{q(y)}{R_{b1}}\sin\nu(y)+\sin\alpha+(\alpha_2-\alpha)\cos\alpha\right]^3}d\alpha + \int_{-\alpha_1}^{-\alpha_g} \frac{3\{1+\cos\alpha_1[(\alpha_2-\alpha)\sin\alpha-\cos\alpha]\}^2(\alpha_2-\alpha)\cos\alpha}{EL\left[\sin\alpha_2-\frac{q(y)}{R_{b1}}\sin\nu(y)+\sin\alpha+(\alpha_2-\alpha)\cos\alpha\right]^3}d\alpha}dy$$

(25)

$$k_s^{\,c} = \int_0^L \frac{1}{\int_{-\alpha_g}^{\alpha_2} \frac{2.4[1+\nu(y)](\alpha_2-\alpha)\cos\alpha\cos^2\alpha_1}{EL\left[\sin\alpha_2-\frac{q(y)}{R_{b1}}\sin\nu+\sin\alpha+(\alpha_2-\alpha)\cos\alpha\right]}d\alpha + \int_{-\alpha_1}^{-\alpha_g} \frac{1.2[1+\nu(y)](\alpha_2-\alpha)\cos\alpha\cos^2\alpha_1}{EL[\sin\alpha+(\alpha_2-\alpha)\cos\alpha]}d\alpha}dy$$

Applying discrete integral method, the stiffness could be calculated by Equations(26) and (27).

(26)

$$k_b^{\,c} = \sum_1^N \frac{1}{\int_{-\alpha_g}^{\alpha_2} \frac{12\{1+\cos\alpha_1[(\alpha_2-\alpha)\sin\alpha-\cos\alpha]\}^2(\alpha_2-\alpha)\cos\alpha}{EL\left[\sin\alpha_2-\frac{q(y)}{R_{b1}}\sin\nu(y)+\sin\alpha+(\alpha_2-\alpha)\cos\alpha\right]^3}d\alpha + \int_{-\alpha_1}^{-\alpha_g} \frac{3\{1+\cos\alpha_1[(\alpha_2-\alpha)\sin\alpha-\cos\alpha]\}^2(\alpha_2-\alpha)\cos\alpha}{EL\left[\sin\alpha_2-\frac{q(y)}{R_{b1}}\sin\nu(y)+\sin\alpha+(\alpha_2-\alpha)\cos\alpha\right]^3}d\alpha}\Delta y$$

(27)

$$k_s^{\,c} = \sum_1^N \frac{1}{\int_{-\alpha_g}^{\alpha_2} \frac{2.4[1+\nu(y)](\alpha_2-\alpha)\cos\alpha\cos^2\alpha_1}{EL\left[\sin\alpha_2-\frac{q(y)}{R_{b1}}\sin\nu(y)+\sin\alpha+(\alpha_2-\alpha)\cos\alpha\right]}d\alpha + \int_{-\alpha_1}^{-\alpha_g} \frac{1.2[1+\nu(y)](\alpha_2-\alpha)\cos\alpha\cos^2\alpha_1}{EL[\sin\alpha+(\alpha_2-\alpha)\cos\alpha]}d\alpha}\Delta y$$

Thus when there exists a cracked tooth on the pinion, the total effective mesh stiffness can be expressed as

$$k_t^{\ c} = \sum_{i=1}^{n} \frac{1}{\frac{1}{k_{h,i}} + \frac{1}{k^{c}_{b1,i}} + \frac{1}{k^{c}_{s1,i}} + \frac{1}{k_{f1,i}} + \frac{1}{k_{a1,i}} + \frac{1}{k_{b2,i}} + \frac{1}{k_{s2,i}} + \frac{1}{k_{a2,i}} + \frac{1}{k_{f2,i}}} \tag{28}$$

From figure 4, it is observed that due to the existence of cracks, the bending and shear stiffness greatly reduces the existence of cracks.

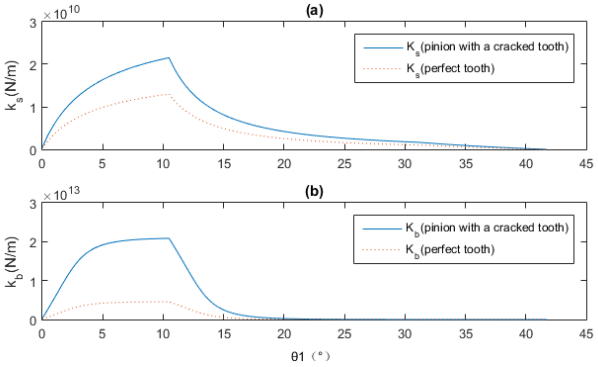

Fig.5. (a) The shear stiffness ks vs. the angular displacement θ1; (b) The bending stiffness kb vs. the angular displacement θ1

The influences spread over the mating duration of the creaked pinion. The total mesh stiffness decreases appreciably due to the crack within the double tooth pair mesh duration. Form Figure 5, We can see that there has been a significant reduction in mesh stiffness.

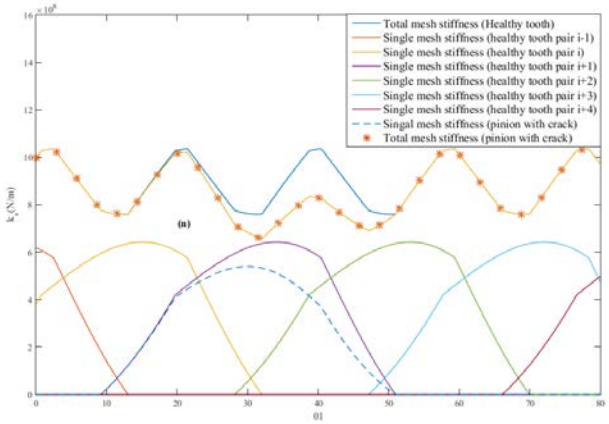

Fig.6. Single and total mesh stiffness

3. Conclusions

This paper presents an analytical method for analyzing the effects of crack on TVMS of helical gears. This study can be used to determine the quantitative relationship between TVMs and gears with tooth crack. However, other factors, such as expanded tooth contact, corrected rounded foundation stiffness, multi tooth meshing area and nonlinear contact stiffness, do not consider more efforts in this work, which is our future work.

Acknowledgements

he financial sponsorship from the project of National Natural Science Foundation of China (51475098, 61463010 and 51405093) and Guangxi Natural Science Foundation (2016GXNSFFA380008) are gratefully acknowledged. It is also sponsored by Guangxi key laboratory of manufacturing system & advanced manufacturing technology (15-140-30-001Z, 16-380-12-004Z, 16-380-12-011K, and 14-045-15-006Z), Innovation Project of Guangxi Graduate Education (YCSW2017136) and basic ability promotion project for young and middle-aged teachers in Guangxi Province (Grant No. 2017KY0207).

References

[1] D.C.H. Yang, J.Y. Lin, Hertzian damping, tooth friction and bending elasticity in gear impact dynamics, J. Mech. Transm-T. ASME 109 (1987) 189–196.

[2] X. Tian, M.J. Zuo, K. Fyfe, Analysis of the vibration response of a gearbox with gear tooth faults, ASME international mechanical engineering congress and exposition, Anaheim, California, USA, 2004.

[3] S. Wu, M.J. Zuo, A. Parey, Simulation of spur gear dynamics and estimation of fault growth, J. Sound Vib. 317 (3) (2008) 608–624.

[4] Sainsot P.Velex P. Duverger O. Contribution of gear body to tooth deflections-A new bidimensional analytical formula, J. Mech. Des. 126(4): 748-752.

[5] X. Zhou, Y. Shao, Y. Lei, M.J. Zuo, Time-varying meshing stiffness calculation and vibration analysis for a 16DOF dynamic model with linear crack growth in a pinion, J. Vib. Acoust. 134 (2012) 1–11.

[6] Z. Chen, Y. Shao, Mesh stiffness calculation of a spur gear with tooth profile modification and tooth root crack, Mech. Mach. Theory 62 (2013) 63–74.

[7] R. Ma, Y. Chen, Research on the dynamic mechanism of the gear system with local crack and spalling failure, Eng. Fail. Anal. 26 (2012) 12–20.

[8] Z. Wan, H. Cao, Y. Zi, et al., Mesh stiffness calculation using an accumulated integral potential energy method and dynamic analysis of helical gears, Mech. Mach. Theory 92 (2015) 447–463.

[9] Han L, Qi H. Influences of tooth spalling or local breakage on time-varying mesh stiffness of helical gears[J]. Engineering Failure Analysis, 2017, 79: 75-88.

[10] Tian X. Dynamic simulation for system response of gearbox including localized gear faults[D]. University of Alberta, 2004.